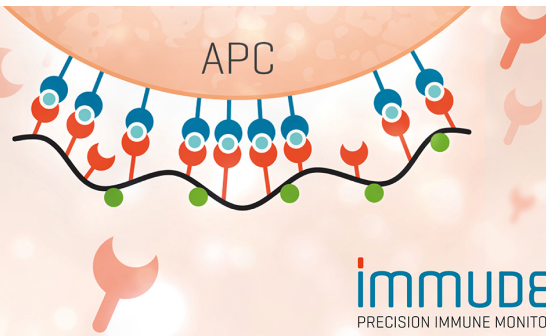


TCR Solutions Detect Antigen Presentation

- Immunex produces your TCRs
- Soluble TCRs and TCR Dextramer®



IMMUDEx[®]
PRECISION IMMUNE MONITORING

The Journal of Immunology

RESEARCH ARTICLE | APRIL 15 2000

Fine Mapping of *IGAD1* in IgA Deficiency and Common Variable Immunodeficiency: Identification and Characterization of Haplotypes Shared by Affected Members of 101 Multiple-Case Families ¹² **FREE**

Igor Vořechovský; ... et. al

J Immunol (2000) 164 (8): 4408–4416.

<https://doi.org/10.4049/jimmunol.164.8.4408>

Related Content

Fine-Scale Mapping at *IGAD1* and Genome-Wide Genetic Linkage Analysis Implicate *HLA-DQ/DR* as a Major Susceptibility Locus in Selective IgA Deficiency and Common Variable Immunodeficiency

J Immunol (March,2003)

A Putative Susceptibility Locus on Chromosome 18 Is Not a Major Contributor to Human Selective IgA Deficiency: Evidence from Meiotic Mapping of 83 Multiple-Case Families

J Immunol (August,1999)

MHC Susceptibility Genes to IgA Deficiency Are Located in Different Regions on Different HLA Haplotypes

J Immunol (October,2002)

Fine Mapping of *IGAD1* in IgA Deficiency and Common Variable Immunodeficiency: Identification and Characterization of Haplotypes Shared by Affected Members of 101 Multiple-Case Families

Igor Vořechovský,^{*†} Michael Cullen,[‡] Mary Carrington,[‡] Lennart Hammarström,^{*} and A. David B. Webster[†]

To limit the region containing a mutation predisposing to selective IgA deficiency (IgAD) and common variable immunodeficiency (CVID), 554 informative members of 101 multiple-case families were haplotyped at the *IGAD1* candidate locus in the MHC. Microsatellite markers were placed onto the physical map of *IGAD1* to establish their order and permit rapid haplotype analyses. Linkage analysis of this extended family set provided additional support for a strong susceptibility locus at *IGAD1* with a maximum multipoint nonparametric linkage score in excess of 3. Although the transmission of maternal *IGAD1* haplotypes from unaffected heterozygous parents to the affected offspring was in excess, this was not apparent in multiple-case families with a predominance of affected mothers, suggesting that this parental bias is influenced by the affection status of transmitting parents and supporting a maternal effect in disease susceptibility. Of 110 haplotypes shared by 258 affected family members, a single haplotype (H1) was found in 44 pairs of affected relatives, accounting for the majority of the *IGAD1* contribution to the development of IgAD/CVID in our families. The H1 allelic variability was higher in the telomeric part of the class III region than in the distal part of the class II region in both single- and multiple-case families. Incomplete H1 haplotypes had most variant alleles in the telomeric part of the analyzed region in homozygous IgAD/CVID patients, whereas this was not observed in unaffected homozygotes. These data suggest that a telomeric part of the class II region or centromeric part of the class III region is the most likely location of *IGAD1*. *The Journal of Immunology*, 2000, 164: 4408–4416.

Immunoglobulin A deficiency (IgAD)³ is the most frequent primary immunodeficiency in humans (1). Affected individuals lack IgA in serum and mucosal secretions and may suffer from susceptibility to infections (1). IgAD shares a putative MHC-linked genetic defect with common variable immunodeficiency (CVID), a more severe disorder of Ig production characterized by a lack of IgG, IgA, and often IgM (2–4).

Numerous case-control studies of this multifactorial disorder have previously shown HLA associations (2, 5–12), suggesting the

existence of a predisposing locus or loci in this region. Further support for the presence of a susceptibility mutation(s) in the MHC (designated *IGAD1*) awaited the evidence for genetic linkage as a significantly increased allele sharing in affected individuals and positive family-based allelic associations, as demonstrated by transmission disequilibrium tests (TDT) (4). TDTs reduce the confounding effect of the population structure on putative allelic associations in case-control studies and should be positive only if the genetic linkage is present (13).

Although a number of allelic associations were reported in IgAD/CVID using serology, RFLP, PCR using sequence-specific oligonucleotide primers (PCR-SSP), and microsatellite markers, no reliable haplotype data have been available that would permit fine mapping of the *IGAD1* locus. Fine mapping of *IGAD1* would facilitate a search for a genuine predisposing mutation(s), but this has been hindered by a high gene density in the region, excessive polymorphism, lower than average recombination fractions and several hot spots for meiotic crossover events in the MHC. The location of *IGAD1* in the class III region has been supported by the observed absence of IgAD among 43 Sardinian DR3 homozygotes who share class II but not class III alleles with the IgAD-associated Northern European haplotype (14). The same region has been favored by an earlier family study (15). A recent analysis of ancestral haplotypes in a large kindred with three CVID patients, three cases with IgAD, and two cases with lower IgA levels (16) suggested that the region between the class III microsatellites designated 821/823 (17) and the HLA-B locus contained the susceptibility gene. However, fine mapping of complex genetic traits based on putative ancestral haplotype fragments shared by few affected family members, some of them with an intermediate phenotype of partial IgA

^{*} Department of Biosciences at NOVUM, Karolinska Institute, Huddinge, Sweden; [†]Medical Research Council Immunodeficiency Research Group, Department of Clinical Immunology, University College London Medical School, London, United Kingdom; and [‡]Biological Carcinogenesis and Development Program, National Cancer Institute-Frederick Cancer Research and Development Program, Frederick, MD 21702

Received for publication December 3, 1999. Accepted for publication February 11, 2000.

The costs of publication of this article were defrayed in part by the payment of page charges. This article must therefore be hereby marked *advertisement* in accordance with 18 U.S.C. Section 1734 solely to indicate this fact.

¹ This study was supported by the Swedish and British Medical Research Councils, the Swedish Strategic Research Foundation, the Primary Immunodeficiency Association of the United Kingdom MSMT VS96097, the Karolinska Institute, and federal funds from the National Cancer Institute, National Institutes of Health, under Contract NO1-CO-56000. The content of this publication does not necessarily reflect the views or policies of the Department of Health and Human Services, nor does mention of trade names, commercial products, or organizations imply endorsement by the U.S. Government.

² Address correspondence and reprint requests to Dr. Igor Vořechovský, Department of Biosciences at NOVUM, Karolinska Institute, CBT Hälsövägen 7, SE-14157 Huddinge, Sweden. E-mail address: igvo@sntp.biosci.ki.se

³ Abbreviations used in this paper: IgAD, selective IgA deficiency; CVID, common variable immunodeficiency; TDT, transmission disequilibrium test; NPL, nonparametric linkage; PCR-SSP, PCR using sequence-specific oligonucleotide primers.

Table I. List of oligonucleotide primer sequences, allelic sizes, and annealing temperatures

Marker Locus	Forward Sequence (5'-3')	Reverse Sequence (5'-3')	T _a (°C)	Size (bp)
7-8601	CCA AGA ACC CAG CAT TC	TTG GGG AAG GAT TCT AAA TAG	55	144–160
6-38576	CAT TAT TTC AAA CTT CCA ACC	CAG CCT CTT ATC ATC CCT AC	55	190–230
9-99431	AAG AAA GTA CCT TAA ATA AAG	CTG TTG CAT GAG TAA AC	55	222–240
8-105224	GCT TAT TCC AGT TCA AGG TC	CAT GGG TTT TCT TTG TGT ATT	55	229–255
11-36252	CTC CAC CCT GGG TGA CAG ACT	GGG CCC TGA ATA CAC CCT TC	55	114–128
15-47549	ATG GGG CAG GTA AAA ACA TCC	GGC CCC CTG TAA GCA GAA C	65	240–280
17-86995	CAG TTC CTC CAG GAC TTA GTA	GAG TTC GCA CCA CTG TAG T	55	256–260
19-162236	TTG CAC CTG ACC AAT TT	CAG GCT AAT GGA AAA CAC TAT	55	250–285
21-8631	TGC TGT CCA ATT CAG GAT ACT	GCG CCA CTG CAC TTG A	65	248–276
22-38114	AAA AGG ACG AAA ATG ACA CA	GGC TTG GGG GAC TAT GA	55	218–238
24-140297	GAG GTC AAA GCT GCA GTA	TAA CAA AAG CTC CCT TCA CT	55	212–234
AB59840	AAA TGG GCA AGA CTT CAA T	TAA TTT TTA GAG GAA TCA CCA	60	292–316
AB73694	AGC TCA TTG CAG GCT CCA ACT	TGT GGT TTA TGC CCG TAA TCT	60	265–295
AB121571	GCC CGA GCA CAG AAA GTG G	AAG AAG GAA TCA TAC CAA AC	60	281–303

deficiency, may not be reliable. A single affected family member with a different haplotype fragment does not necessarily limit the *IGAD1* locus and the excess sharing of an IgAD/CVID-associated MHC haplotype in affected heterozygotes may suggest a location of *IGAD1* centromeric to the *821/823* locus (16). Although the relative risk of developing IgAD conferred by the homozygous B8-DR3 haplotype was estimated to be as high as 75 (16), screening of 30 Scandinavian B8-DR3 homozygotes did not reveal any IgAD (L. Hammarström et al., manuscript in preparation), indicating a lower risk. A central MHC location for *IGAD1*, which contains genes coding for products influencing Ab production, including complement proteins (18), has been disputed by pointing to a primary association of IgAD with *DQB1*0201* (19). The proposal of neutral amino acids of the codon 57 in the DQ β chain as the only major MHC determinant of IgAD susceptibility has not been accepted (11, 20), and there is currently no consensus where the *IGAD1* gene/mutation maps. Although the ability to induce IgAD in vivo by a group of lysosomotropic agents suggests some interference with Ag-processing events (4), this provides little clue to the exact *IGAD1* location because a number of closely linked MHC genes play a role in Ag presentation and T cell activation.

Successful fine mapping of predisposing mutations underlying complex genetic traits requires a sufficient collection of well-characterized families and accurate genotyping of family members followed by haplotype analyses. The construction of haplotypes has been hampered by the costs of DNA-based typing for HLA specificities associated with unequal probabilities of determining correctly each allele in heterozygotes. Although easy-to-type genetic markers such as simple sequence repeats may help, meiotic mapping over short genetic distances cannot establish their reliable order to permit valid haplotype analyses.

In this study, we show a physical map of *IGAD1* microsatellites, single tube PCR-based genetic markers that detect both alleles in heterozygotes with more equal probability than DNA-based typing for HLA specificities. The placement of novel and previously reported microsatellite loci onto the physical map, now represented by an MHC sequence (21), allowed us to determine their correct order and to carry out a rapid and inexpensive haplotype analysis of our collection of 101 multiple-case European families with IgAD/CVID. To narrow down the *IGAD1* locus, we have identified and characterized haplotypes shared by 258 affected pedigree members, analyzed their allelic variability, and suggested the likely location of a susceptibility mutation. We also report two families carrying a crossover event in the *IGAD1* candidate region in informative meioses and provide the estimate of the class II and class III recombination fraction in our family material. In addition,

we propose that the observed parental allele transmission bias to IgAD/CVID offspring is influenced by the maternal phenotype/genotype, supporting a maternal effect in disease susceptibility. Finally, a nonparametric genetic linkage analysis and family-based associations on this extended set of families provide further support that *IGAD1* is a strong susceptibility locus for the most prevalent human Ig deficiencies.

Materials and Methods

Family material

The complete set of 101 multiple-case pedigrees is at http://www.cbt.ki.se/fam/set3-7/scan_set.html. The ascertainment of probands and family members was described previously (4, 22). The families were recruited through the European Society for Immunodeficiency Registry in Sweden ($n = 49$) and the U.K. ($n = 34$). Samples from small multiple-case families were obtained from Italy ($n = 4$), the Czech Republic ($n = 3$), The Netherlands ($n = 2$), Belgium ($n = 1$), Turkey ($n = 1$), Finland ($n = 2$), Poland ($n = 1$), Russia ($n = 2$), and Spain ($n = 2$). Single-case families were from Sweden and the U.K.

Genotyping

Genotyping at microsatellite loci was conducted using fluorescent-labeled primers on an ABI 377-Sequencer using the Genescan 672 and Genotyper software packages (Applied Biosystems Division, Perkin-Elmer, Norwalk, CT). The primer sequences used for amplifying novel or previously reported microsatellite loci are shown in Table I. HLA typing at *HLA-B*, *DRB1*, *DQA1*, and *DQB1* loci was performed using PCR-SSP as described previously (8). Family MHC recombinants were further analyzed using microsatellites at *DNRNG4031* (23), *G272258* (5'-CTT GCC AAT GGA ATG TGA GC-3', 5'-GAG ACA AAC ACT GAA GCC TC-3'), and *DQCAR* (24). These loci were typed with radioactively labeled oligonucleotide primers as previously described (25). The genetic or physical map for a subset of the marker loci used in the present study was described earlier (26, 27) or is shown in Fig. 1.

Linkage analysis

A total of 554 pedigree members from 101 apparently unrelated multiplex families were analyzed for linkage, consisting of 258 affected, 231 unaffected and 65 family members with unknown phenotype (http://www.cbt.ki.se/fam/set3-7/scan_set.html). The family material contained 94 affected pairs of siblings, 41 unaffected sib pairs, and 8 half-sibs. Only 30 affected children had affected fathers as compared with 118 affected children with unaffected fathers. In contrast, and in line with our previously described parent-of-origin penetrance effect (4), 75 IgAD/CVID children were born to affected mothers as compared with 95 affected children born to the unaffected mothers, a proportion more than doubled in our family material (http://www.cbt.ki.se/fam/set3-7/scan_set.html). Allele numbers at each locus, their population frequencies, observed heterozygosity, and polymorphism information content are shown at <http://www.cbt.ki.se/fam/mhcgdat.htm>. Full genotypes of all family members are shown at <http://www.cbt.ki.se/fam/mhcre.htm>. Nonparametric linkage (NPL) analysis was

Nucleotide sequence with accession numbers

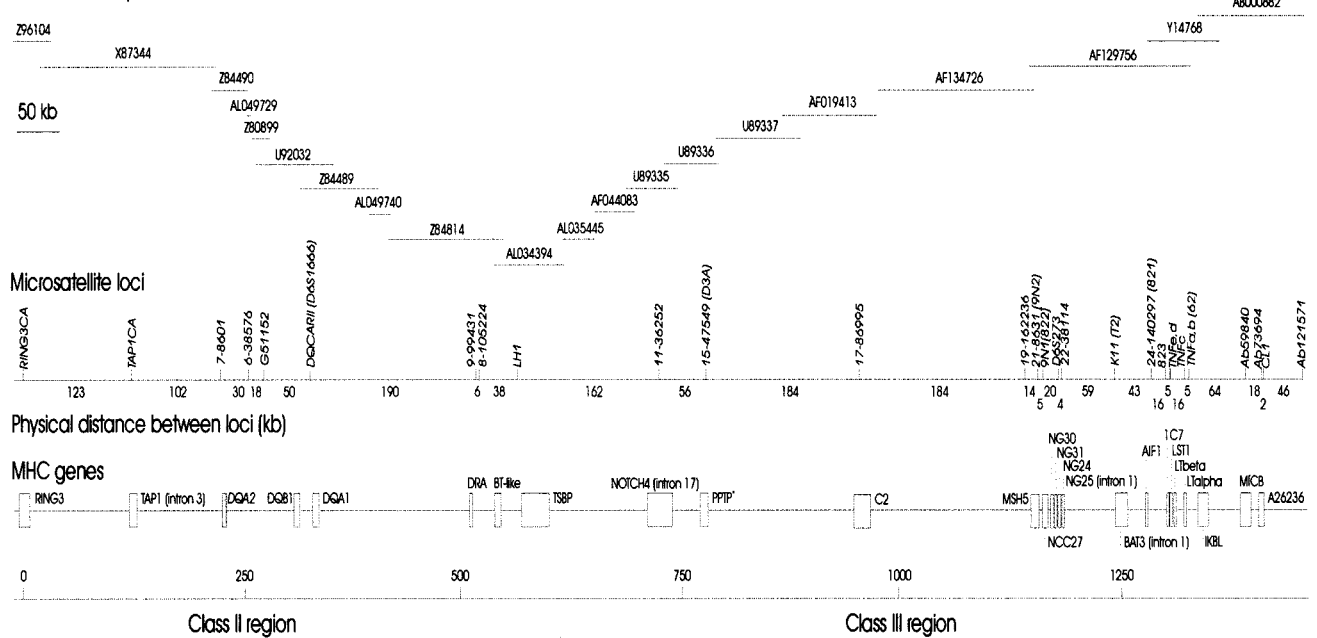


FIGURE 1. Microsatellite loci on the physical map of the *IGAD1* candidate region. The GenBank/EMBL accession numbers are shown above nucleotide sequences represented by dotted lines. Map distances are drawn to scale and reflect a particular haplotype sequenced. The distances vary on different haplotypes due to extensive insertion/deletion polymorphisms. Only those MHC genes relevant to the position of microsatellite markers are shown. The oligonucleotide primers amplifying previously unreported loci, or novel primers used for the detection of known simple sequence repeats, are shown in Table I. The references to the remaining microsatellite loci are as follows: *RING3CA*, *G51152* (33); *TAP1CA* (34, 35); *DQCARI* (27, 36); *LHI*, *9N1*, *9N2*, *821*, *823*, *62* (17); *K11* (37); *D6S273* (26); *TNF* (38); *CL1* (39). The microsatellites *822* and *9N1* were previously reported as two different loci (16, 17) amplifying discordant alleles in the same cell lines (17); however, we found that *822* and *9N1* represent the same repeat. *PPTP* is a gene similar to palmitoyl-protein thioesterase precursor in *Bos taurus* (GenBank accession number U89336) with yet unknown function. Loci *11-36252*, *Ab73694*, and *17-86995* showed limited heterozygosity.

conducted with a unified multipoint approach implemented in the Genehunter program available at <http://waldo.wi.mit.edu/ftp/distribution/software/genehunter/gh2/> (28). The Genetic Analysis System (<ftp://ftp.ox.ac.uk/pub/users/ayoung>) was used for converting Genotyper peak labels into allele numbers and analyzing parental allelic segregation differences.

The ascertainment of the family material used for TDT was described previously (4). A total of 109 single-case-father-mother trios were analyzed together with 13 families containing 2 affected offspring and 1 family with 3 affected offspring. All index cases included in TDT had only unaffected parents as determined by repeated nephelometric measurements of serum Ig levels (4).

Haplotype analysis

Haplotypes were constructed using a maximum-likelihood method implemented in the Genehunter (28). Haplotypes of all family members are available as a Genehunter output file at <http://www.cbt.ki.se/fam/mhchaplo.htm>. Haplotypes were inspected and corrected manually against the Genotyper plots. Families with different H1 haplotype fragments in the *IGAD1* candidate region were retyped to exclude genotyping errors and confirm variant alleles.

Results

Physical map of microsatellite loci in the *IGAD1* candidate region

To facilitate haplotype analysis of *IGAD1*, oligonucleotide primers flanking simple sequence repeats were designed and tested for polymorphisms and mendelian inheritance using a panel of 12 DNA samples from different ethnic populations (Caucasian, African, Mongoloid) and 3 families. Novel polymorphic loci (Table I) and those previously reported were placed on to the physical map (Fig. 1) available as a contiguous overlapping sequence in public databases. The map covers the *IGAD1* candidate region in the

olomeric part of the MHC class II region and the class III region (Fig. 1). The map will facilitate a rapid and inexpensive haplotype analysis of large numbers of individuals and will be useful in genetic studies of MHC-linked complex traits, including a number of autoimmune diseases.

Genetic linkage of *IgAD/CVID* to MHC in 101 multiple-case families with *IgAD/CVID*

The results of NPL analysis on the extended family sample are shown in Tables II and III. Single-point analyses were significant for closely linked markers located in or flanking the MHC. Multipoint analyses showed maximum NPL/ Z_{lr} scores in excess of 3 at about 5.6 cM telomeric of *D6S1610* for both the pairs of affected family members and all informative individuals (Table III). Higher NPL/ Z_{lr} scores were observed for affected pairs of relatives as compared with all individuals informative for linkage, possibly reflecting an effect of unknown age-dependent penetrance. These results further strengthen the evidence for genetic linkage with this extended sample of families.

Identification of haplotypes shared by 258 affected members of multiple-case families

Altogether, 110 haplotypes were shared by at least 2 affected members of multiple-case families. Maximum likelihood haplotypes for all analyzed pedigree members are shown at <http://www.cbt.ki.se/fam/mhchaplo.htm>.

The most common haplotype, designated H1, was shared by 44 pairs of affected family members (Table IV). Shared H1 haplotypes showed virtually no allelic variability at *G51152* and *DQCARI* loci (Table IV). In contrast, the *RING3* gene located just

Table II. Results of nonparametric linkage analysis of 101 IgAD/CVID families: single-point NPL analysis^a

Marker Locus	NPL _{all} (p)	Z _{lr-all} (LOD _{lr})	NPL _{pairs} (p)	Z _{lr-pairs} (LOD _{lr})	α, HLOD	Information Content
<i>D6S1610</i>	1.37 (0.05)	2.05 (0.92)	1.40 (0.05)	2.07 (0.93)	0.34, 0.41	0.52
<i>D6S291</i>	1.56 (0.03)	2.58 (1.44)	1.72 (0.02)	2.72 (1.61)	0.19, 0.06	0.51
<i>D6S1583</i>	2.97 (0.0003)	4.08 (3.49)	3.21 (0.0001)	4.33 (4.13)	0.49, 1.19	0.68
<i>RING3CA</i>	1.81 (0.02)	2.58 (1.45)	2.10 (0.006)	2.94 (1.88)	0.37, 0.68	0.63
<i>G51152</i>	2.19 (0.005)	3.10 (2.13)	2.43 (0.002)	3.41 (2.52)	0.50, 1.14	0.63
<i>DQCARI</i>	2.65 (0.001)	3.40 (2.51)	2.78 (0.0007)	3.47 (2.61)	0.40, 0.78	0.75
<i>9N2</i>	2.29 (0.004)	3.11 (2.10)	2.50 (0.001)	3.28 (2.34)	0.41, 0.78	0.71
<i>9N1</i>	1.24 (0.07)	2.14 (0.99)	1.30 (0.06)	2.13 (0.98)	0.45, 0.60	0.50
<i>D6S273</i>	1.40 (0.05)	1.96 (0.84)	1.60 (0.04)	2.36 (1.21)	0.12, 0.03	0.67
<i>821</i>	1.24 (0.07)	1.84 (0.74)	1.46 (0.04)	2.10 (0.95)	0.33, 0.44	0.62
<i>62</i>	1.73 (0.02)	2.28 (1.13)	1.96 (0.01)	2.52 (1.37)	0.26, 0.31	0.68
<i>D6S1558</i>	0.25 (0.38)	0.40 (0.07)	0.44 (0.30)	0.68 (0.10)	0.01, 0.00	0.50
<i>D6S1621</i>	0.94 (0.14)	1.44 (0.45)	1.26 (0.07)	1.84 (0.73)	0.11, 0.01	0.56
<i>D6S461</i>	0.54 (0.26)	0.92 (0.19)	0.58 (0.25)	0.97 (0.20)	0.15, 0.12	0.48

^a NPL score, α (proportion of *IGAD1*-linked families) and HLOD (heterogeneity LOD score) was as previously defined (28); Z_{lr} score was described by Kong and Cox (32). The scores were computed for pairs of affected pedigree members only (pairs) and for all family members (all) using the Genehunter 2 (28) and Genehunter Plus 1.2 algorithms (32).

over 0.25 megabase proximal of *G51152*, was represented by four alleles, indicating the centromeric border of *IGAD1* (Fig. 1). The most common *RING3* allele 3 (231 bp) was found on 27 of 44 H1 haplotypes, with alleles 2, 4, 5, and 6 found on 5, 7, 4, and 1 occasions, respectively (Table IV). Although there was no such obvious telomeric border in the class III region, the allelic variability at the central MHC loci between *9N2* and *TNF* was higher than that at the *G51152-DQCARI* region, with a variant allele(s) in 12 families (Table IV). Seven of 12 families with variant H1 alleles/haplotypes in *IGAD1* were Swedish, whereas families cv82 and cv114 with a variant allele at *D6S273* came from Northern Italy and families cv131, cv135, and cv145 were from the British Isles (Table IV). A number of families with different haplotype fragments at the telomeric part contrasted with a single variant allele in the distal part of the class II region in one family (Table IV), despite the highest observed heterozygosity, polymorphism information content, and allele number at *DQCARI* (<http://www.cbt.ki.se/fam/mhcghdat.htm>). Although the families with variant H1 alleles did not come from a single population, a number of Swedish families sharing identity-by-descent H1 haplotype with positive NPL scores (cv6, cv18, cv15, cv107 in Table IV) support a distal part of the class II region rather than the previously proposed telomeric part of the class III region as containing an *IGAD1* mutation.

Although parental samples of the affected siblings in the Swedish family cv15 (Table IV) were not available, additional family members including their unaffected siblings and the offspring could be typed using markers *TAP1CA*, *7-8601*, *8-105224*, *LH1*, *11-36252* and *17-86995* (Fig. 1). These results indicated that the

affected siblings shared only a centromeric part of the H1 haplotype up to a recombination event in a 40-kb region between *8-105224* and *LH1*, whereas a distal part contained different alleles (Table IV). Furthermore, these class III alleles were strongly negatively associated with the disease in both the single- and multipoint TDT of our family material (data not shown). This family suggests that *IGAD1* is centromeric to the *LH1* locus.

Representative carriers of the most commonly shared haplotypes were typed using PCR-SSP at *HLA-B*, *DRB1*, *DQB1*, and *DQA1* loci. The H1 haplotype was invariably found to contain disease-associated alleles *HLA-DQB1*02*, *HLA-DRB1*03*, and *HLA-DQA1*05* (Table IV). Haplotype H2 (alleles 244–200 bp at the *G51152-DQCARI* loci, respectively; *HLA-DQB1*05*, *DQA1*01*, *DRB1*01*) was identified in 18 affected H1/H2 individuals. Multipoint TDT analysis revealed 28 transmissions vs 13 nontransmissions from parents heterozygous for this haplotype, confirming previously identified allelic associations in case-control studies (1) in a family-based design. Haplotype H3 (alleles 226–192 bp at *G51152-DQCARI*; *HLA-DQB1*02*, *DQA1*03*) was identified in 4 affected homozygotes and 18 H1/H3 heterozygotes with IgAD/CVID; however, multipoint and single-point TDT analysis showed no significant excess of transmissions of this haplotype/allele. Haplotype H4 (alleles 214–216 bp at *G51152-DQCARI*; *HLA-DQB1*03*, *DQA1*02*, *DRB1*07*) was found in 10 heterozygous H1/H4 carriers. Although multipoint TDT suggested an excess of transmissions vs nontransmissions from heterozygous parents (25 vs. 16), single-point TDT was negative for each allele (26 vs 23 for the 216-bp allele at *DQCARI*, 47 vs 64 for the 214-bp allele at *G51152*).

Haplotypes H1-H4 were found in the majority of affected family members. Ninety-nine of 258 affected family members possessed only haplotypes H1-H4 at the *G51152-DQCARI* loci, while an additional 113 carried one of the four haplotypes, giving a total of 82% (212/258) affected pedigree members carrying at least one of these haplotypes. This figure suggests a restricted repertoire of the MHC molecules in affected individuals and further strengthens the role of the MHC locus in IgAD/CVID susceptibility.

Homozygosity at the *IGAD1* locus

Typing of 101 multicase families using markers at and flanking the MHC region (Fig. 1, Tables I and VI) identified a total of 16 carriers of the associated haplotype H1 homozygous at *G51151*, *DQCARI*, *9N1*, *9N2*, *D6S273*, *821*, and *62*. All representative

Table III. Results of nonparametric linkage analysis of 101 IgAD/CVID families: Multipoint NPL analysis^a

Score	All Individuals (θ)	Pairs of Affected Members (θ)
NPL _{max} , significance (p)	3.049 (5.6), 0.0002	3.196 (5.6), 0.00009
Z _{lr-max}	3.545 (5.6)	3.656 (5.6)
LOD _{lr-max}	2.728 (5.6)	2.902 (5.5)
Information content at θ _{max}	0.926	0.926

^a θ, genetic distance in centimorgans from the *D6S1610* locus; NPL score, α (proportion of *IGAD1*-linked families) and HLOD (heterogeneity LOD score) was as previously defined (28); Z_{lr} score was described by Kong and Cox (32). The scores were computed for pairs of affected pedigree members only and for all family members using the Genehunter 2 (28) and Genehunter Plus 1.2 algorithms (32).

Table IV. H1 haplotypes shared in 101 multiple-case families with IgAD/CVID^a

Family	NPL	Relationship	RING3	G5I152	DQB1	DQCARI1	DQA1	DRB1	9N2	9N1	D6S273	821	62	HLA-B	D6S1558
cv1	0.63	AS, PO	3	216	02 02	202	-	03 03	253	98	140	212	148	08 27	7
cv6	1.4	AS	3	216	-	202	-	-	251	98	140	212	148	-	7
cv8	-0.5	PO	5	216	-	202	-	-	253	98	140	212	148	-	7
"	"	AS	3	216	-	202	-	-	255	98	140	212	148	-	6
cv5	0.69	AS, PO	3	216	-	202	-	-	-	98	140	212	148	-	7
cv10	0	AS	6	216	-	202	-	-	253	98	140	212	148	-	7
cv18	0.96	AS	4	216	02 05	202	0101 0501x5	03 01	253	98	140	212	146	35 40	9
"	"	PO	3	216	-	202	-	-	253	98	140	212	148	-	7
cv61	1.76	AS, PO	3	216	-	202	-	-	253	98	140	212	148	-	7
cv4	0.6	AS, PO	4	216	-	202	-	-	253	98	140	212	148	-	6
cv9	1.34	AS, PO	2	216	-	202	-	-	253	98	140	212	148	-	9
cv15	1.4	AS	3	214/216	02 03	196/202	0302 0501x5	03 09	265/267	96/98	134/138	216/224	164/156	08 08	7/9
cv16	1.4	AS	3/2	216/218	02 05	198/202	-	03 14	253/265	98/96	136/140	212/216	148/164	07 08	7/9
cv22	0.01	AS	3	216	-	202	-	-	253	98	140	212	148	-	7
cv24	1.4	AS	3	216	-	202	-	-	253	98	140	212	148	-	0
cv29	1.4	AS	3	216	-	202	-	-	253	98	140	212	148	-	7
cv31	0	PO	4	216	-	202	-	-	253	98	140	212	148	-	7
cv32	1.1	AS	3	216	-	202	-	-	253	-	140	-	148	-	3
cv55	1.4	AS	5	216	-	202	-	-	253	98	140	212	148	-	7
"	"	"	2	216	-	202	-	-	253	98	140	212	148	-	7
cv56	0.37	AS	3	216	-	202	-	-	253	98	140	212	148	-	7
cv73	1.41	AS	3	214/216	02 03	202	0201 0501	03 07	253	98	140	212	148	08 39	7
cv93	1.41	AS	3	216	-	202	-	-	253	98	140	212	148	-	6
cv94	1.41	AS	3	214/216	02 03	202	0201 0501	03 07	253	98	140	212	148	08 39	7
cv34	0.59	AS, PO	3	216	-	202	-	-	-	98	140	212	148	-	7
cv36	0	PO	3	216	02 02	202	0501 0501	03 09	-	102	138	232	168	07 40	7
cv75	1.73	PO	3	216	-	202	-	-	253	-	140	212	148	-	7
cv79	0.93	AS	3	216	-	202	-	-	98	140	212	148	-	6	
cv82	1.41	AS	3	216	-	202	-	-	253	98	138	212	148	-	7
cv130	0	PO	3	216	-	202	-	-	253	98	140	212	148	-	7
cv134	-0.4	AS, not P	3	216	-	202	-	-	253	98	140	212	148	-	6
cv135	0.44	AS, not P	5	216	-	202	-	-	253	100	140	212	148	-	7
cv42	2.4	AS, PO	4	216	02 05	202	0104 0501x5	03 14	-	98	140	212	148	08 14	7
cv37	1.41	AS	2	216	-	202	-	-	-	98	140	212	148	-	3
cv38	0	PO	4	216	-	202	-	-	-	98	140	212	148	-	4
cv41	0	PO	2	216	-	202	-	-	-	102	140	212	148	-	9
cv46	1.9	AS	3	216	-	202	0101 0501x5	03 01	-	98	140	212	148	08 27	7
cv97	-0.7	AS	3	216	-	202	-	-	-	98	140	212	148	-	7
cv114	1.41	AS	4	216	-	202	-	-	253	98	142	212	148	-	6
cv107	1.24	AS, PO	3	216	02 02	200/202	0201 0501x5	03 07	253	98	140	212	156	08 44	9
cv118	1.41	AS	4	216	-	202	-	-	253	98	140	212	148	-	7
cv144	0	PO	3	216	-	202	-	-	-	98	140	212	148	-	9
cv131	0	PO	3	216	02 03	204	0201 0501x5	03 07	253	98	140	212	164	07 57	7
cv145	2.39	AS	5	216	-	202	-	-	253	98	140	212	146	-	6/7

^a Each row represents an H1 haplotype or its variant shared by a pair of affected family members. Variant portions of H1 haplotypes are boxed. AS, haplotype shared by affected siblings; PO, haplotype shared by affected parent and affected offspring; P, parent. A slash between allelic sizes indicates unknown linkage phase. Each representative H1 carrier analyzed for HLA specificities at *DQB1*, *DQA1*, and *DRB1* invariably had a genotype with at least one allele 02, 05, and 03, respectively, whereas the HLA-B locus showed variant alleles. Unknown alleles or genotypes are designated with -.

family members typed for HLA specificities using PCR-SSP were found to be homozygous for *DQB1**02, *DRB1**03, *DQA1**05 alleles. Of 16 homozygotes, 6 family members from altogether 4 families were unaffected, whereas 9 cases from 6 families had IgAD and 1 patient had CVID. However, seven more affected (six IgAD and one CVID) cases, but only one unaffected family member (homozygous in the class III, but not in the class II region, data not shown), were homozygous for H1 alleles in at least two loci (Table V). Similarly, haplotyping of single case-parent trios revealed two homozygous IgADs and one homozygous CVID carrier of the full H1 haplotype. In addition, two affected index cases were found to carry this haplotype with a variant allele at the 62 or *DQCARI1* loci (Table V).

These data indicate that the affected homozygotes carrying a portion of the H1 haplotype shared common alleles at the telomeric region of the class II region, while possessing variant haplotype fragments at the telomeric part of the class III region (Table V and Fig. 1). This pattern corresponded to the H1 haplotypes shared by heterozygous individuals (Table IV). These results

suggest that the *IGAD1* mutation is at the centromeric part of the class III region or in the telomeric part of the class II region.

Identification of class II and class III recombinants

The recombinant families were detected in the process of genome-wide linkage mapping of 83 multiple-case families containing a total of 449 pedigree members, 215 of them affected (I.V. et al., manuscript in preparation). Initially, seven families were identified with recombinant meioses between the proximal *D6S1583* and distal *D6S461* marker loci, located about 6 cM apart and flanking the MHC (26). These families were typed using a set of closely spaced markers within the MHC to identify those with a recombination event in the *IGAD1* candidate region. Two such families were found, giving a recombination fraction estimate of 0.4% (2 of 501 meioses) in the proximal half of the MHC (~2 × 10⁶ bp). Fine mapping of the crossover in family cv29 placed the breakpoint telomeric of *TNFD*, whereas in family cv5 the markers *DNRNG4031* and *DNRNGCA* (25) placed the crossover to a 4-kb area between the *HLA-DNA* and *RING3* genes (data not shown), a region that contains

Table V. Shared incomplete H1 haplotypes of family members homozygous for at least two loci in multiple-case (A) and single-case families (B)^a

Family	Family Member	Diagnosis	RING3	G51152	DQCARI1	9N2	9N1	D6S273	821	62	
A	Cv10	Mother	IgAD	231/233	216	202	253	98	140	212	148
			IgAD	231/233	216	202	253	98	140	212	148
		Sib A	IgAD	231/233	216	202	253	98	140	212	148
				231/233	216	202	253	98	136	212	158
	Sib B	Nonaffected	231/233	222	198	253	100	136	216	154	
			231/233	216	202	253	98	140	212	148	
	Cv18	Mother	CVID	231	216	202	253	98	140	212	148
				229	244	200	259	96	134	216	156
		Father	Nonaffected	0	0	0	0	0	0	0	0
				233	216	202	253	98	140	212	146
		Sib A	IgAD	231	216	202	253	98	140	212	148
				233	216	202	253	98	140	212	146
	Sib B	IgAD	231	216	202	253	98	140	212	146	
			229	244	200	259	96	134	216	156	
	Cv22	Sib A	CVID	231	216	202	253	98	140	212	148
				231	216	202	255	100	136	216	154
		Sib B	IgAD	231	216	202	253	98	140	212	148
				235	244	200	255	100	134	214	146
Cv36	Parent	IgAD	231	216	202	0	102	138	224	168	
			233	226	192	0	98	134	214	164	
	Offspring	IgAD	231	216	202	0	102	138	224	168	
Cv134	Sib A	IgAD	229	216	202	0	98	140	212	148	
			231	216	202	253	98	140	212	148	
	Sib B	IgAD	235	214	196	265	102	128	224	164	
			231	216	202	253	98	140	212	148	
	Sib C	Nonaffected	229	222	198	253	98	140	212	148	
			229	222	198	253	98	140	212	148	
			229	226	192	267	96	136	214	164	
B	Tdt41	Offspring	IgAD	233	216	202	77	98	140	155	148
				233	216	202	77	98	140	155	156
	Tdt62	Offspring	IgAD	233	216	202	77	98	140	155	148
				229	216	204	77	98	140	155	148

^a A slash between allelic sizes indicates unknown linkage phase; unknown loci or haplotypes are designated by zero; different portions of H1 haplotype are boxed in dark gray; haplotypes different from the H1 haplotype are in light gray. All variant genotypes have been confirmed by repeated typing.

a hot spot for recombination events (25). Although there were both affected and unaffected descendants of recombinant and nonrecombinant meioses, making each family potentially informative for narrowing the location of a predisposing mutation, the cosegregation of phenotypes and haplotypes provided no conclusive evidence as to the location of *IGAD1*.

Transmission-disequilibrium analysis

The single-point TDT showed the most significant transmission distortion at *DQCARI1* in multiple-case families (Table VI). In single-case families, the most significant disequilibrium was observed for a negatively associated allele at *LH1* and the 216-bp allele at *G51152* (Table VI); the latter allele was found on all H1 haplotypes shared by affected family members (Table IV). The *G51152* and *DQCARI1* loci showed association with more than one allele/haplotype: the H1 haplotype (alleles 216–202 bp, respec-

tively) was transmitted on 36 occasions whereas it was retained 17 times in single-case families; these numbers were 48 and 24, respectively, in multiple-case families. The number of transmissions vs. nontransmissions for the H2 haplotype 244–200 (226–200) was 25/13 (7/2) in single-case families and 28/13 (12/4) in multiple-case families. The telomeric part of class III or centromeric part of class II region showed the most significant family-based allelic associations of all markers in both the single- and the multicase pedigrees.

Parental bias in transmission of IgAD-associated alleles is influenced by parental affection status

The TDT analysis using a large set of single-case families with unaffected parents was conducted separately for each parental transmission. In accordance with our previously reported data (4), we found a bias in the transmission of maternal vs paternal alleles/

Table VI. Maternal and paternal transmission of MHC alleles in unaffected parents-affected offspring trios and multiple-case families^a

Marker Locus	Allele (bp)	Both Parents (T/NT (χ^2 , p))	Maternal Source (T/NT)	Paternal Source (T/NT)
Unaffected parents-affected offspring trios				
<i>RING3</i>	232	41/25 (3.9, 0.05)	22/11	14/12
<i>G51152</i>	216	53/23 (11.9, 0.0006)	30/9	21/13
<i>DQCAR</i>	200	32/18 (3.9, 0.05)	14/8	15/8
	202	36/20 (4.6, 0.03)	22/8	12/10
	<i>192</i>	15/36 (8.7, 0.003)	8/19	5/11
<i>LH1</i>	77	42/23 (5.6, 0.02)	23/8	16/14
	<i>91</i>	39/75 (11.4, 0.0007)	20/38	18/33
<i>9N1</i>	98	75/52 (4.2, 0.04)	42/18	25/24
<i>D6S273</i>	140	43/22 (6.8, 0.009)	20/7	18/14
	<i>136</i>	41/55 (2.0, 0.15)	15/22	19/23
<i>K11</i>	155	36/24 (2.4, 0.12)	16/6	18/14
	149	52/25 (9.5, 0.002)	27/8	23/17
	157	27/13 (4.9, 0.03)	16/7	11/4
Multiple-case families				
<i>RING3</i>	232	62/33 (8.9, 0.003)	21/16	24/14
<i>G51152</i>	216	54/37 (3.2, 0.07)	19/23	19/8
<i>DQCAR</i>	200	38/15 (10.0, 0.002)	19/8	16/5
	202	62/29 (12.0, 0.0005)	22/19	21/10
<i>9N2</i>	253	59/29 (10.2, 0.002)	20/16	19/11
<i>9N1</i>	98	61/43 (3.1, 0.08)	26/20	20/17
	<i>96</i>	16/36 (7.7, 0.006)	7/10	6/15
<i>D6S273</i>	140	49/23 (9.4, 0.002)	17/14	16/8
	<i>136</i>	35/63 (8.0, 0.005)	12/16	20/30
<i>821</i>	212	53/26 (9.2, 0.002)	18/14	18/7
<i>62</i>	149	55/38 (3.1, 0.08)	15/17	20/14
	157	23/15 (1.7, 0.19)	12/5	8/7

^a T, NT, number of transmissions and nontransmissions from heterozygous parents to the affected offspring; p values were defined in the Genehunter program (28). Alleles with excess of transmissions are in bold; alleles with excess of nontransmissions are in italics. Only completely genotyped trios were included for the analysis of parental bias.

haplotypes from unaffected heterozygous parents to the affected offspring (Table VI). In multiple-case families, we also found a significant TDT for most *IGAD1* loci studied, although no clear parental bias was observed. This suggests that the parental transmission bias of associated *IGAD1* alleles to the affected offspring is influenced by the parental phenotype. Because affected mothers transmitting the phenotype to the offspring are overrepresented as compared with affected male transmitters in our data set, it is the maternal phenotype that is likely to contribute more to this effect.

Discussion

Location of *IGAD1*

The results of our present study suggest that the most likely location of the IgAD/CVID susceptibility mutation is in the telomeric part of the class II region or centromeric part of the class III region. This is supported by 1) the most significant family-based allelic associations in the class II loci in TDT (Table VI) and in previous case-control studies (8, 29); 2) the allelic uniformity at *DQCARI*, and particularly at *G51152* on the H1 haplotype, which shows the most significant association with IgAD/CVID in the population studied; 3) the existence of variant H1 haplotypes in the telomeric part of the class III region in a number of heterozygous multiple-case families, which are shared in excess by the affected family members; 4) the allelic variability of haplotype fragments at the telomeric part of *IGAD1* in affected H1 homozygotes as compared with the centromeric part; and 5) no such bias in nonaffected individuals.

Although our data do not support the previously suggested class III location for the IgAD/CVID susceptibility gene (14–16), we believe that they do not warrant the exclusion of the suggested region between the *G1* gene and the *821/823* loci. Fine mapping of susceptibility loci in complex traits cannot be reliably based on a

single or even a few ancestral recombination events because the phenotype in such families may have been determined by different etiological factors. Although there were many more families with variant H1 fragments in the previously implicated class III region than in the opposite part of *IGAD1* (Tables IV and V), the shared haplotype may not have been a major susceptibility factor for the development of the phenotype in a particular family. This uncertainty is magnified by zero or negative NPL scores in some families with a variant H1 haplotype, their diverse population of origin and a possibility that a single variant allele in a number of H1 haplotypes could have arisen due to a marker locus mutation rather than an ancestral recombination event (Table IV). However, the existence of several Swedish families with clear ancestral H1 variants and positive NPL scores does provide a support for the telomeric part of the class II region rather than the telomeric end of the class III region (Table IV). A dense coverage of the candidate disease loci with markers followed by linkage disequilibrium analyses in general pedigrees using recently introduced methods may prove to be useful for mapping disease loci in suitable populations even in the MHC. Although a locus heterogeneity and putative genetic interaction between more than one predisposing MHC loci is speculative, it cannot be excluded, in particular if there are a number of genes in the region implicated in T-cell activation.

Contribution of *IGAD1* to IgAD/CVID

What is the strength of the MHC locus and its relative contribution to the IgAD/CVID susceptibility? Assuming a penetrance ratio of 20, a dominant model, and a frequency of disease allele of 0.1%, ~40% of families showed linkage to the MHC, contributing to the heterogeneity LOD score of ~1.36. With a phenocopy rate of 1% and penetrance ratio of 80, the proportion of MHC-linked families in our sample would drop to about 23%. However, if the number

of phenocopies is higher and the disease penetrance is lower, the contribution of the MHC to the overall disease prevalence could exceed 40% (e.g., 3% phenocopies and 40% IgAD/CVID penetrance in our families would raise this estimate to 49% under the same mode of inheritance). Although it will be interesting to assess the contribution of the MHC more accurately using the data of our genome-wide scan with multiple-case families (I. Vořechovský, L. Hammarström, A. D. B. Webster, et al., manuscript in preparation), it is becoming increasingly apparent that *IGAD1* is a major susceptibility locus for common human Ig deficiencies.

Role of *IGAD1* homozygosity in susceptibility to IgAD/CVID

At least six H1 homozygotes were identified among nonaffected family members, indicating that mere H1 homozygosity at the candidate *IGAD1* loci is not sufficient for the development of IgAD/CVID and that additional factors must exist in the pathogenesis of the defect. However, the number of H1 homozygotes including H1 variants was almost tripled in affected individuals, possibly suggesting a role in IgAD/CVID predisposition via a putative recessive defect. Although we were not able to type all family members for HLA specificities because of the costs incurred, these results appear to correspond to those of de la Concha et al. (30), who reported an increased number of class II homozygotes among CVID patients. However, this increase may not be a primary contributor to the disease susceptibility due to a restricted diversity of class II molecules as proposed (30) but could reflect the presence of a genuine predisposing mutation in close proximity to the class II genes. This has been observed in a number of families with recessive mendelian disorders and utilized for the autozygosity mapping of underlying disease genes. The support for mere *IGAD1* homozygosity as an important etiological factor in IgAD/CVID susceptibility is further diminished by zero or negative NPL values in families with homozygous H1 carriers (Tables V and VI).

Family MHC recombinants

The discovery of disease genes has often been facilitated by the identification of informative multiple-case families with a short cut event such as a cytogenetic abnormality, microdeletion, gene conversion, or informative crossover. IgAD exhibits a high relative risk to siblings, supporting a limited number of predisposing loci (4), and strong familial clustering can therefore make these events informative also in multifactorial disorders. However, both such families in our data set proved to be uninformative in this respect.

In the first family, affected siblings shared both MHC haplotypes identical by descent, but only one full and one recombinant haplotype with a nonaffected sister and nonaffected brother, respectively, consistent with an increased allelic sharing of affected individuals and linkage to the MHC. Assuming the presence of an IgAD-predisposing mutation on the maternally inherited haplotype shared by affected sisters, full penetrance of the mutation in this family, and no *trans*-acting influence of the paternally inherited haplotype in the son, the location of *IGAD1* would be compatible with the class III region distal to the recombination event between *MIB* and *TNFD* loci. This area would correspond to that suggested by haplotype analysis of a large family with CVID (16), further limiting the proposed candidate region on its centromeric side by more than 20 kb, excluding *IC7* and a centromeric part of the *LST1* gene. However, if *IGAD1* were present on the paternally inherited IgAD-associated haplotype, the family would provide no information about the location of *IGAD1*.

In the second family, containing six affected individuals in two generations, affected daughters shared the IgAD-associated haplotype HLA-B8-D6S273(140)-DR17-DQ2. However, there was no co-segregation of the haplotype with the phenotype in the subse-

quent generation, arguing for the presence of non-MHC determinants in IgAD susceptibility. Thus, even if IgAD confers a high risk of developing the defect in close relatives, potentially informative family recombinants failed to provide conclusive evidence for the *IGAD1* location. These examples illustrate difficulties in fine mapping complex disease genes.

TDT in the analysis of parental allelic effects

While single-case-unaffected parent trios showed an excess of the transmission of maternal haplotypes to the affected offspring (Table VI), this was not obvious in multiple-case families with a predominance of IgAD-transmitting mothers (Table VI), although the overall positivity of TDT was clearly observed for both ascertainment schemes. Unlike case-control studies, TDT can distinguish maternal and fetal genotype effects (31) by considering separately maternal genotypes with both maternal grandparents first and then, in a second step, fetal-parental trios. In addition to the impact of the gender of transmitting parents on the phenotypic outcome of the offspring (4), our present study supports the hypothesis that it is also a maternal MHC genotype that influences the risk of IgAD in the offspring. Our results also suggest that the parental phenotype of index cases should be considered when designing pedigree structures for genetic studies on human complex traits with parental allelic bias in susceptibility loci and/or parent-of-origin penetrance differences.

Acknowledgments

We thank J. Björkander, T. Español, C. M. Farber, L. Gomez, S. Koskinen, M. D. Laycock, J. Litzman, J. Lokaj, L. Luo, N. Matamoros, C. Mullighan, R. Paganelli, E. Pařízková, A. Plebani, I. Quinti, A. Ryan, O. Sanal, H. Siwinska-Golebiowska, M. N. Voniatis, C. M. R. Weemaes, and P. L. Yap for referring families with IgAD/CVID or technical help.

References

- Burrows, P. D., and M. D. Cooper. 1997. IgA deficiency. *Adv. Immunol.* 65:245.
- Schaffer, F. M., J. Palermos, Z. B. Zhu, B. O. Barger, M. D. Cooper, and J. E. Volanakis. 1989. Individuals with IgA deficiency and common variable immunodeficiency share polymorphisms of major histocompatibility complex class III genes. *Proc. Natl. Acad. Sci. USA* 86:8015.
- Volanakis, J. E., Z.-B. Zhu, F. M. Schaffer, K. J. Macon, J. Palermos, B. O. Berger, R. Go, R. D. Campbell, H. W. J. Schroeder, and M. D. Cooper. 1992. Major histocompatibility complex class III genes and susceptibility to immunoglobulin A deficiency and common variable immunodeficiency. *J. Clin. Invest.* 89:1914.
- Vořechovský, I., A. D. B. Webster, A. Plebani, and L. Hammarström. 1999. Genetic linkage of IgA deficiency to the major histocompatibility complex: evidence for allele segregation distortion, parent-of-origin penetrance differences and the role of anti-IgA antibodies in disease predisposition. *Am. J. Hum. Genet.* 64:1096.
- Ambrus, M., E. Hernadi, and G. Bajtai. 1977. Prevalence of HLA-A1 and HLA-B8 antigens in selective IgA deficiency. *Clin. Immunol. Immunopathol.* 7:311.
- Hammarström, L., and C. I. Smith. 1983. HLA-A, B, C and DR antigens in immunoglobulin A deficiency. *Tissue Antigens* 21:75.
- Cobain, T. J., M. A. French, F. T. Christiansen, and R. L. Dawkins. 1983. Association of IgA deficiency with HLA A28 and B14. *Tissue Antigens* 22:151.
- Olerup, O., C. I. Smith, J. Björkander, and L. Hammarström. 1992. Shared HLA class II-associated genetic susceptibility and resistance, related to the *HLA-DQB1* gene, in IgA deficiency and common variable immunodeficiency. *Proc. Natl. Acad. Sci. USA* 89:10653.
- Fiore, M., C. Pera, L. Delfino, I. Scotese, G. B. Ferrara, and C. Pignata. 1995. DNA typing of DQ and DR alleles in IgA-deficient subjects. *Eur. J. Immunogenet.* 22:403.
- Mullighan, C. G., G. C. Fanning, H. M. Chapel, and K. I. Welsh. 1997. TNF and lymphotoxin- α polymorphisms associated with common variable immunodeficiency: role in the pathogenesis of granulomatous disease. *J. Immunol.* 159:6236.
- Reil, A., G. Bein, H. K. G. Machulla, B. Sternberg, and M. Seyfarth. 1997. High-resolution DNA typing in immunoglobulin A deficiency confirms a positive association with DRB1*0301, DQB1*02 haplotypes. *Tissue Antigens* 50:501.
- Howe, H. S., A. K. L. So, J. Farrant, and A. D. B. Webster. 1991. Common variable immunodeficiency is associated with polymorphic markers in the human major histocompatibility complex. *Clin. Exp. Immunol.* 83:387.
- Schaid, D. J., and S. S. Sommer. 1994. Comparison of statistics for candidate-gene association studies using cases and parents. *Am. J. Hum. Genet.* 55:402.

14. Cucca, F., Z. B. Zhu, A. Khanna, F. Cossu, M. Congia, M. Badiali, R. Lampis, F. Frau, S. De Virgiliis, A. Cao, et al. 1998. Evaluation of IgA deficiency in Sardinians indicates a susceptibility gene is encoded within the HLA class III region. *Clin. Exp. Immunol.* 111:76.
15. Wilton, A. N., T. J. Cobain, and R. L. Dawkins. 1985. Family studies of IgA deficiency. *Immunogenetics* 21:333.
16. Schroeder, H. W., Jr., Z. B. Zhu, R. E. March, R. D. Campbell, S. M. Berney, S. A. Nedospasov, R. L. Turetskaya, T. P. Atkinson, R. C. Go, M. D. Cooper, and J. E. Volanakis. 1998. Susceptibility locus for IgA deficiency and common variable immunodeficiency in the HLA-DR3, -B8, -A1 haplotypes. *Mol. Med.* 4:72.
17. Hsieh, S.-L., R. March, A. Khanna, S. J. Cross, and R. D. Campbell. 1997. Mapping of 10 novel microsatellites in the MHC class III region: application to the study of autoimmune disease. *J. Rheumatol.* 24:220.
18. French, M. A., and R. L. Dawkins. 1990. Central MHC genes, IgA deficiency and autoimmune disease. *Immunol. Today* 11:271.
19. Olerup, O., C. I. Smith, and L. Hammarström. 1991. Is selective IgA deficiency associated with central HLA genes or alleles of the DR-DQ region? *Immunol. Today* 12:134.
20. French, M., R. Dawkins, F. T. Christiansen, W. Zhang, M. A. Degli-Esposti, and G. Saueracker. 1991. Is selective IgA deficiency associated with central HLA genes or alleles of the DR-DQ region? Reply. *Immunol. Today* 12:135.
21. Consortium. 1999. Complete sequence and gene map of a human major histocompatibility complex. *Nature* 401:921.
22. Vofechovský, L., H. Zetterquist, R. Paganelli, S. Koskinen, A. D. Webster, J. Björkander, C. I. Smith, and L. Hammarström. 1995. Family and linkage study of selective IgA deficiency and common variable immunodeficiency. *Clin. Immunol. Immunopathol.* 77:185.
23. Cullen, M., J. Noble, H. Erlich, K. Thorpe, S. Beck, W. Klitz, J. Trowsdale, and M. Carrington. 1997. Characterization of recombinants in the HLA class II region. *Am. J. Hum. Genet.* 60:397.
24. Macaubas, C., J. Hallmayer, J. Kalili, A. Kimura, S. Yasunaga, F. C. Grumet, and E. Mignot. 1995. Extensive polymorphism of a (CA)_n microsatellite located in the HLA-DQA1/DQB1 class II region. *Hum. Immunol.* 42:209.
25. Cullen, M., H. Erlich, W. Klitz, and M. Carrington. 1995. Molecular mapping of a recombination hotspot located in the second intron of the human TAP2 locus. *Am. J. Hum. Genet.* 56:1350.
26. Dib, C., S. Faure, C. Fizames, D. Samson, N. Drouot, V. A., P. Millasseau, S. Marc, J. Hazan, E. Seboun, M. Lathrop, et al. 1996. A comprehensive genetic map of the human genome based on 5264 microsatellites. *Nature* 380:152.
27. Martin, M. P., A. Harding, Chadwick, R., M. Kronick, M. Cullen, L. Lin, E. Mignot, and M. Carrington. 1998. Characterization of 12 microsatellite loci of the human MHC in a panel of reference cell lines. *Immunogenetics* 47:131.
28. Kruglyak, L., M. J. Daly, M. P. Reeve-Daly, and E. S. Lander. 1996. Parametric and nonparametric linkage analysis: a unified multipoint approach. *Am. J. Hum. Genet.* 58:1347.
29. Olerup, O., C. I. Smith, and L. Hammarström. 1990. Different amino acids at position 57 of the HLA-DQ β chain associated with susceptibility and resistance to IgA deficiency. *Nature* 347:289.
30. De La Concha, E. G., M. Fernandez-Arquero, A. Martinez, F. Vidal, P. Vigil, L. Conejero, M. C. Garcia-Rodriguez, and G. Fontan. 1999. HLA class II homozygosity confers susceptibility to common variable immunodeficiency (CVID). *Clin. Exp. Immunol.* 116:516.
31. Mitchell, L. E. 1998. Differentiating between fetal and maternal genotypic effects using transmission test for linkage disequilibrium. *Am. J. Hum. Genet.* 60:1006.
32. Kong, A., and N. J. Cox. 1997. Allele-sharing models: LOD scores and accurate linkage tests. *Am. J. Hum. Genet.* 61:1179.
33. Beck, S., S. Abdulla, R. P. Alderton, R. J. Glynn, I. G. Gut, L. K. Hosking, A. Jackson, A. Kelly, W. R. Newell, P. Sanseau, et al. 1996. Evolutionary dynamics of non-coding sequences within the class II region of the human MHC. *J. Mol. Biol.* 255:1.
34. Beck, S., A. Kelly, E. Radley, F. Khurshid, R. P. Alderton, and J. Trowsdale. 1992. DNA sequence analysis of 66 kb of the human MHC class II region encoding a cluster of genes for antigen processing. *J. Mol. Biol.* 228:433.
35. Carrington, M., and M. Dean. 1994. A polymorphic dinucleotide repeat in the third intron of TAP1. *Hum. Mol. Genet.* 3:218.
36. Lin, L., L. Jin, A. Kimura, M. Carrington, and E. Mignot. 1997. DQ microsatellite association studies in three ethnic groups. *Tissue Antigens* 50:507.
37. Colonna, M., G. B. Ferrara, J. Strominger, and T. Spies. 1991. Hypervariable microsatellites in the central MHC class III region. In *HLA 1991*. K. Tsuji, M. Aizawa, and T. Sasazuki, eds. Oxford University Press, Oxford, p. 179.
38. Udalova, I. A., S. A. Nedospasov, G. C. Webb, D. D. Chaplin, and R. L. Turetskaya. 1993. Highly informative typing of the human TNF locus using six adjacent polymorphic markers. *Genomics* 16:180.
39. Ulgiati, D., G. Grimsley, C. Leelayuwat, and L. J. Abraham. 1996. Analysis of the major histocompatibility complex microsatellite CL1 in different human haplotypes. *Eur. J. Immunogenet.* 23:205.